MASTER'S DEGREE THESIS

# Interuniversity Master in Statistics and Operations Research

**Title: Structural Equation Models for the estimation of functional connectivity in fMRI brain signal**

**Author: Núria Mancho-Fora**

**Advisor: Joan Guàrdia-Olmos, Ph. D., and Ernest Pons-Fanals, Ph. D.**

**Department: Departament de Metodologia de les Ciències del Comportament**

**University: Universitat de Barcelona**



UNIVERSITAT POLITÈCNICA DE CATALUNYA
BARCELONATECH
Facultat de Matemàtiques i Estadística

UNIVERSITAT DE BARCELONA

Universitat Politècnica de Catalunya
Facultat de Matemàtiques i Estadística

Master's Thesis

# Structural Equation Models for the estimation of functional connectivity in fMRI brain signal

*Author:*
Núria Mancho Fora

*Supervisors:*
Dr. Joan Guàrdia Olmos
Dr. Ernest Pons Fanals

*A thesis submitted in fulfilment of the requirements*
*for the degree of Master's degree of Statistics and Operations Research*
*developed in the*

Grup de Tècniques Estadístiques Avançades Aplicades a la Psicologia
Departament de Metodologia de les Ciències del Comportament
Universitat de Barcelona

October 6, 2014

UNIVERSITAT POLITÈCNICA DE CATALUNYA

# *Abstract*

Facultat de Psicologia
Departament de Metodologia de les Ciències del Comportament
Universitat de Barcelona

Master's degree of Statistics and Operations Research

**Structural Equation Models for the estimation of functional connectivity in fMRI brain signal**

by Núria Mancho Fora

An incresing number of contributions in Quantitative an Computational Neuroscience have stressed that cognitive processes should be understood as a complex network of segregated brain areas. Among these contributions, functional connectivity studies the covariance over time among segregated brain regions that compound a functional network. This work aims to analyse the application of Structural Equation Models (SEM) to represent complex networks in brain connectivity, and explore the challenges in the application of these models in this particular context.

**Methods**. The sample consisted of two groups of 12 participants, matched by age, with high and low spelling skills (HSS and LSS, respectively). During an fMRI session, two different block-design experiments involving homophone spelling Spanish language were applied to each group. In the first task, individuals were asked assess the presence or absence of an homophone orthographic error. While in the second task, they were asked to detect the presence or absence of an "i" in the word presented, regardless of the spelling.

**Results**. First, a descriptive analysis of the Regions of Interest in each condition is provided, and after this the fit indexes and parameter of the Structural Equation Models estimated in each condition and group are reported.

**Conclusions**. This work has permitted to identify certain issues in the application of SEM to functional connectivity research.

**Keywords**: Structural Equation Modeling, functional magnetic resonance, functional connectivity, brain signal.

UNIVERSITAT POLITÈCNICA DE CATALUNYA

# *Resum*

Facultat de Psicologia
Departament de Metodologia de les Ciències del Comportament
Universitat de Barcelona

Master's degree of Statistics and Operations Research

**Structural Equation Models for the estimation of functional connectivity in fMRI brain signal**

by Núria Mancho Fora

Un creixent nombre de contribucions en Neurociència Quantitativa i Computacional han assenyalat que els processos cognitius haurien de ser entesos com un xarxa complexa d'àrees cerebrals segregades. Entre aquestes contribucions, la connectivitat funcional estudia la covariància al llarg del temps de regions segregades del cervell que componen xarxes funcionals. Aquest treball té per objectiu analitzar l'aplicació de Models d'Equacions Estructurals (SEM) per representar xarxes complexes en conectivitat cerebral, així com explorar els possibles reptes de l'aplicació dels SEM en aquest context particular.

**Mètode**. La mostra va consistir en dos grups de 12 participants, aparellats per edat, amb alta i baixa competència ortogràfica (HSS i LSS respectivament). Durant una sessió de fMRI, dos experiments diferents en disseny de blocks es van aplicar a cada grup. En la primera tasca, es va demanar als individus que avaluessin la presència o absència d'un error homòfon d'ortografia. Mentre que en la segona tasca se'ls va demanar que detectessin la presència o absència d'una "i" en la paraula presentada, sense tenir en compte l'ortografia.

**Resultats**. En primer lloc, es proporciona una anàlisi descriptiva de les Regions cerebrals d'Interès i a continuació, es presenten els índex d'ajust i les estimacions dels paràmetres dels Models d'Equacions Estructurals per cada condició experimental i grup.

**Conclusions**. Aquest treball ha permès identificar alguns reptes en l'aplicació de SEM a l'estudi de la connectivitat funcional.

**Paraules clau**: Models d'equacions estructurals, ressonància magnètica funcional, connectivitat funcional, senyal cerebral.

# *Acknowledgements*

This work would have never been possible without the constant support of an extensive network of people.

First of all, I want to extend my appreciation to Dr. Joan Guàrdia-Olmos and Dr. Maribel Peró-Cebollero for their guidance and continuous assistance, as well as their untiring revisions, but most of all for their trust along these years.

In like manner, I kindly thank Dr. Ernest Pons-Fanals for his valuable orientation along this master's programme.

Thirdly, I wish to thank the rest of the GTEAAP and my colleges for their contributions, as well as for sharing their enthusiasm for the study of brain and behaviour.

This would not be complete without thanking my parents for encouraging me to define and pursue my aims, my two brothers for sharing with me their passion for science, and Eric for being a source of support and stoically coping with my constantly being involved in new projects.

Last but not least, I would like to thank all those who have had the patience to become participants in this research.

# Contents

# List of Figures

# List of Tables

# Abbreviations

| | |
|---|---|
| **fMRI** | **f**unctional **M**agnetic **R**esonance **I**maging |
| **BOLD** | **B**lood **O**xigen **L**evel **D**ependent |
| **ROI** | **R**egion **O**f **I**nterest |
| **HSS** | **H**igh **S**pelling **S**kills group |
| **LSS** | **L**ow **S**pelling **S**kills group |

*Regions of Interest:*

| | |
|---|---|
| **LCPL** | **L**eft **C**erebellum, **P**osterior **L**obule |
| **LITG** | **L**eft **I**nferior **T**emporal **G**yrus |
| **LMFG** | **L**eft **M**iddle **F**rontal **G**yrus |
| **LPCG1** | **L**eft **Pre**central **G**yrus [1] |
| **LPCG2** | **L**eft **Pre**central **G**yrus [2] |
| **LPHG** | **L**eft **Para**h**i**ppocampal **G**yrus |
| **LRAC** | **L**eft-**R**ight **A**nterior **C**ingulate |
| **LRMFG** | **L**eft-**M**iddle **F**rontal **G**yrus |
| **RMTG** | **R**ight **M**iddle **T**emporal **G**yrus |
| **RPCG** | **R**ight **Pre**central **G**yrus |
| **RSFG** | **R**ight **S**uperior **F**rontal **G**yrus |
| **RSMG** | **R**ight **Supra**m**a**rginal **G**yrus |

# Chapter 1

# Introduction

Connectivity research field studies the interactions between different areas of the brain with the objective of inferring models for brain networks, and explaining how those interactions depend on the experimental conditions. Such issues are major concerns for Quantitative and Computational Neuroscience and are approached through both research and simulation studies.

Several techniques provide information about brain activity, yet in the recent years functional Magnetic Resonance Imaging (fMRI, hereafter) has taken a prominent role in this scientific field. Although hindered by a low temporal resolution, this non-invasive technique offers higher spatial resolution that makes it advantageous in both clinical and research settings. Specific features of this technique will be dealt with in Chapter 2.

Whenever fMRI is combined with an experimental design that presents sequences of stimuli to individuals, it allows the researchers to measure changes in brain activation when one or more independent variables are manipulated. This measurements will permit testing previously stated research hypotheses about psychological, neural, or haemodynamic processes [19].

Therefore, fMRI studies have contributed to characterize functional specialization within brain areas, which is known as *functional segregation*, where researches aim to establish statistical dependencies between experimental manipulations and brain responses [11, 12]. However, in the recent decades there has been a steady growth in interest towards describing how various brain regions connect and interact in sophisticated systems, as well as explaining those interactions [29], which is known as *functional integration*. This

approach stresses the idea that cognitive processes depend on interactions between brain regions, and not solely on the activation within separated brain areas [39].

The complex nature of those reciprocal effects hinders their assessment and, in order to approach this problem, literature in the field distinguishes between *anatomical*, *functional*, and *effective connectivity* [8, 12, 29, 41].

Anatomical connectivity focuses on describing how different brain areas are physically linked, whereas functional connectivity studies regional undirected association at a macro level. That is, it studies the covariance over time among segregated brain regions that may compound a functional network [39]. Multivariate statistical methods are used to compare correlations between Regions of Interest (ROIs) [29]. For instance, Principal Component Analysis and Independent Component Analysis allow to identify task-related patterns of brain activation without making any a priory assumptions.

Related to effective connectivity, it deals with studying the influence that a neural system may exercise over another, attempting to make statements about those causal effects [28, 29]. Amongst the most frequently used techniques in the literature we can highlight *Structural Equation Modelling*, *Dynamic Causal Modelling*, and *Granger Causality Modelling*.

Dynamic Causal Modelling understands the brain as a deterministic non-linear dynamic system that is subject to inputs and produces outputs [10], and it is more tolerant with reciprocal effects [17]. In contrast, Granger Causality Modelling quantifies the capability of past activation values of a ROI to predict the current values in another ROI.

Related to Structural Equation Modelling (SEM, henceforth), it is important to highlight that its malleability has allowed its application to a wide variety of phenomena in several domains of science. In our particular scenario, SEM attempts to explain the variance-covariance structure of a data set, here the activation patterns of previously selected ROIs. The earliest relevant contributions to this subject can mainly be found in the works by McIntosh and González-Lima [30–32], while later McIntosh [33] proposed certain guidelines for the use of SEM in the estimation of brain connectivity.

The computation capacity SEM allows us to identify cognitive processes as a complex series of hierarchically organized computational models, which is consistent with the general formulations of SEM. Moreover, it is assumed that the processes analysed are

usually conceived as separable, and that the final cognitive process is defined by the addition of the partial processes. Furthermore, the estimation of brain connectivity with SEM does not take into consideration the biological structure of the nervous system. Thus, we will take a more conservative approach and refer to functional connectivity as those statistical models formulating stochastic structural relationships between specific brain ROIs that show statistically significant activity when facing certain cognitive tasks [16].

The standard procedure to estimate functional connectivity using SEM can be broadly summarized in the following phases [33]:

1. Selection of regions or nodes of the network driven by a combination of univariate analysis of changes in signal intensity, multivariate analyses and theoretical guidance.
2. Obtaining the anatomical model.
3. Calculation of the interregional covariance o correlations matrix from the fMRI data.
4. Estimation of the path coefficients and comparison of functional models, according to the characteristics of the statistical estimation technique, as well as the properties of observed distributions.

This initial guidelines for the use of SEM in the estimation of functional brain connectivity has been complemented by many contributions that have led this topic to slightly more complex procedures [9, 21, 25, 36, 37, 39, 40].

In addition to this, some extensions to the general model of SEM have been developed, which have generated interesting statistical approximations to the study of connectivity that share the logic of SEM. For instance, some of the relevant contributions are Unified Structural Equation Models [7, 14], or the Extended Unified Structural Equation Models [13, 43], as well as recent procedure by Inman that refines phases in the generation of SEMs for the estimation of functional connectivity [20]. However, as any other technique, neither SEM, nor functional conectivity are except of limitations [2, 21].

All in all, the application of SEM, and related methods, to the study of brain connectivity is nowadays an active topic in Quantitative and Computational Neuroscience, and for

this reason it deserves special consideration. Technical details of SEM will be extensively reviewed in Chapter 3.

## 1.1 Aim of the study

This work purports to analyse the application of Structural Equation Models to represent complex networks in brain connectivity, and explore the difficulties in the application of said models in this particular context.

More specifically, Structural Equation Models will be applied to study the performance of 24 individuals in visual word recognition and homophone orthographic errors in Spanish language.

# Chapter 2

# Functional Magnetic Resonance Imaging: data acquisition and preprocessing

This chapter briefly introduces the object of study and aims to explain key issues regarding how data is obtained and processed before conducting any further analysis.

## 2.1 Blood Oxygen Level Dependent Contrast

Functional Magnetic Resonance is included in a set of techniques, generally known as functional methods [23], that registers changes in brain signal due to the manipulation of independent behavioural variables. In order to do so, fMRI is usually implemented through the Blood Oxygen Level Dependent contrast (BOLD, hereafter), which assumes that since metabolic processes require glucose and oxygen (being supplied through haemoglobin within the red blood cells), then neuronal activity will elicit changes in the vascular system [19].

More specifically, oxyhaemoglobin is normally transformed into deoxyhaemoglobin at a constant rate. Yet, whenever neurons become active, the vascular system provides more oxyhaemoglobin to those neural areas than is actually needed [19]. Given that haemoglobin molecule has different magnetic properties depending on whether or not it

is bound to oxygen, the intensity of those changes elicited by experimental conditions can be measured placing the individuals within a magnetic field and obtaining series of Magnetic Resonance images [5, 19, 29, 44]. Those series of images can be used to infer brain activity.

The shape of BOLD haemodynamic response to a single stimulus depends on both the mode in which stimuli is applied, as well as the haemodynamic response to neural activation [29]. In that sense, BOLD signal, $x(t)$, at time $t$ can be modelled as a convolution of a stimulus function $v(t)$ and an haemodynamic response function $h(t)$ as follows [4, 29]:

$$x(t) = (v \cdot h)(t) \tag{2.1}$$

This property is illustrated in Figure 2.1 for the two experimental designs explained below in this chapter.

Nonetheless, it should be taken into account that there are yet many unknown features regarding how neuronal activity is translated into BOLD signal, since it is an indirect measure of neuronal function [39].

## 2.2 Magnetic Resonance signal generation

Functional Magnetic Resonance uses strong magnetic fields (typically, from 1.5 to 7.0 Tesla) to compose images of brain tissue in order to study changes in brain function over time [19]. During a data collection session, the individuals are placed into this magnetic field while they perform a set of tasks [29].

Magnetic resonance scans construct 3-dimensional images from sets of 2-dimensional slices, whose thickness is determined by scanner parameters. When an image is reconstructed, it is presented as a matrix of signal values.

During an experimental session, whole brain volumes are collected at $T$ separated time points throughout the an experiment, and each of them is compounded by roughly 100,000 homogeneous cubic volumes called *voxels*. Each voxel is a 3-dimensional rectangular prism, whose dimensions are specified by three scanner parameters (field of view, matrix size and slice thickness) [19], that corresponds to an identified spatial location

with uniform activation intensity, which can be tracked across the sequence of brain volumes, producing a time series. Therefore, voxels are the fundamental unit of measure in this research field. Finally, such experimental procedures are usually repeated for $M$ individuals [29].

## 2.3 Spatial and temporal resolution

The term *spatial resolution* refers to the ability to discriminate between two signals when they arise in nearby spatial locations [5]. Magnetic resonance is specially advantageous in terms of spatial resolution, given its ability to provide detailed anatomical scans where gray and white brain tissues can be easily distinguished, and a resolution often below $1mm^3$. However, such accuracy highly increases the costs of a resonance session, and researchers usually work with resolutions on the order of $3 \times 3 \times 5mm^3$ [29].

Another issue that should be taken into account is that whenever data across individuals is obtained, data on their brains are warped onto a standard template brain [29]. Although this normalization procedure allows to work with inter-individual data, activation in small areas can be easily misplaced. However, the application of enhanced preprocessing techniques enables to make those effects less critical.

The ability to accurately represent data is known as *temporal resolution* and it depends on the repetition time, or the time between each individual image. If one considers that (1) neuronal activity takes place mere milliseconds after an external stimulus, and (2) most fMRI studies deal with repetition times between 0.5 and 4 seconds [29], a gap between the object of study and its measurement is evident. Unfortunately, it is currently impossible to maximize both properties and researches must balance them while designing an experiment and choosing the appropriate registering technique.

## 2.4 Experimental designs

Brain connectivity studies are mainly approached through two classes of experimental design: *blocked*, and *event-related designs*. The former type presents the experimental conditions separated into extended time intervals, known as blocks, whereas the latter class of design presents short and discrete stimuli in randomized timings.

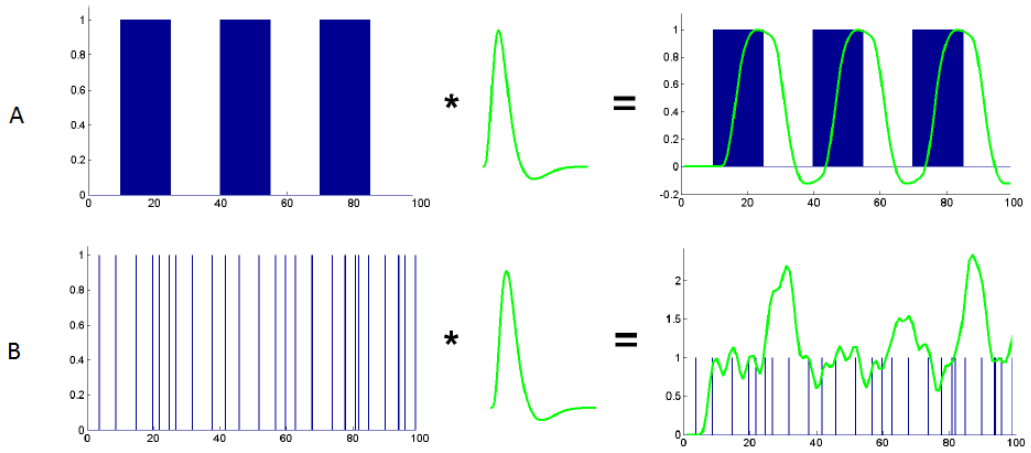


FIGURE 2.1: Diagram of BOLD signal in blocked (A) and event related designs (B) (adapted from Lindquist, 2008)

It must be taken into account that the choice of either experimental design conditions the shape of BOLD haemodynamic response, and therefore any subsequent analysis. Figure 2.1 displays a diagram by Lindquist (2008) of the stimulus functions of a blocked design (A) and an event-related design (B), and how once they are convoluted with the canonical form of the haemodynamic response, it allows to model the BOLD signal.

In addition to this, each of the previously mentioned designs has properties that make them suitable for different types of research questions. Essentially, block designs offer higher detection and estimation power as the length of the blocks is increased, due to the fact that larger blocks lead to larger evoked responses [19, 29]. However, if blocks are too long, it produces a reversed effect due to participants fatigue. In contrast, event-related designs are a suitable option to study phenomenons that are susceptible to fatigue of automatic responses during longer experimental sessions.

The research presented in the current work makes use of blocked designs applied to two different experimental procedures.

## 2.5 Preprocessing of fMRI data

Regardless of the experimental design, once data is obtained, it is necessary to apply a series of computational procedures, generally called *preprocessing*, before conducting any

further analysis. Preprocessing aims to detect and correct, by means of specialized software, problems with fMRI data acquisition so that they do not compromise statistical analysis. More specifically, aims to minimize the influence data acquisition and physiological artefacts, and to standardize the locations of brain regions across individuals [19, 29, 38].

The most frequently applied processes are summarized below:

**Motion correction**

Head motion is one of the most damaging problems in fMRI data acquisition, for a slight movement can drastically change the activation values of the affected voxels, and cause biased changes in their time series. Therefore, motion is estimated and use to correct the orientation of the brain images.

**Normalization**

Whenever collecting data from a group of individuals, it is important to bear in mind that individual brains have slightly different shapes and sizes. Therefore, it must be guaranteed that each voxel lies within the same anatomical structure. Normalization registers each individual brain to a standardized template brain, for instance, the Montreal Neurological Institute coordinate system.

**Spatial smoothing**

This process usually involves convolving the functional images with a Gaussian kernel, which blurs residual anatomical differences, in order to improve inter-subject registration and minimize the effects of spatial normalization.

## 2.6 Data analysis

In order to localize brain activity, one approximation consists in defining brain areas or Regions of Interest (ROI), which can be obtained through different methods such as: manual delimitation, semi-automatic approaches, completely automatic processes, or anatomic atlases. In semi-automatic analysis delimitation software, the technician can interactively adjust intensity thresholds to detect the contours of the ROIs, whereas probability maps are used in completely automatic delimitation.

Whatsoever method might be used, the time series included in each ROI are estimated. In comparison to voxel analysis, ROI based analysis is more robust, since it compensates noise effects across voxels [38].

In the current study, a ROI based functional connectivity analysis was conducted, where ROIs were selected through Principal Component Analysis.

# Chapter 3

# Structural Equation Modelling applied to functional connectivity

Structural Equation Modelling (SEM) refers a wide variety of statistical techniques, from path analysis to generalized latent variable models, and they are also commonly known as *structural analysis of covariances and correlation matrices* [22], or *covariance structure models* [27]. Early developments of these techniques also included the terminology *causal models*, yet in the recent decades less controversial terms have been favoured.

Whenever working in SEM, it is key to distinguish between observed variables and latent variables. The former are those variables that can be made operative and observations can be collected. In contrast, the latter are hypothetical constructs which reflect a non-observable continuum [26]. Observed variables may serve as indirect measures of latent variables, in such case they are referred to as *indicators*. In brief, observed variables admit several response modalities, while latent variables are assumed to be absolutely continuous.

For the purpose of the present study, no latent variables will be considered. Thus, this chapter will present the theoretical framework of SEM observed variables in order to set practical considerations of its application to fMRI brain signal data.

## 3.1 General expression for SEM with observed variables

Structural Equation Models with observed variables aim to explain, by means of linear regression-based models, a vector of endogenous variables with a vector of exogenous variables, while allowing reciprocal relationships [3]. Such models take the expression

$$\boldsymbol{y} = \boldsymbol{B}\boldsymbol{y} + \boldsymbol{\Gamma}\boldsymbol{x} + \boldsymbol{\zeta} \tag{3.1}$$

where

$\boldsymbol{B} = m \times m$ coefficient matrix

$\boldsymbol{\Gamma} = m \times n$ coefficient matrix

$\boldsymbol{y} = p \times 1$ vector of endogenous, dependent, variables

$\boldsymbol{x} = q \times 1$ vector of exogenous, independent, variables

$\boldsymbol{\zeta} = p \times 1$ vector of random errors in the equations

It is generally assumed that the errors ($\boldsymbol{\zeta}$) are uncorrelated with $\boldsymbol{x}$, and that $\boldsymbol{x}$ and $\boldsymbol{y}$ represent the latent variables exactly (for instance, $\boldsymbol{\xi}_{n\times 1}$ and $\boldsymbol{\eta}_{m\times 1}$ respectively). Therefore, the number of $y$ variables equals the number of $\eta$ variables ($p = m$), and the number of $x$ variables equals the number of $\xi$ variables ($q = n$).

SEM can be classified into two major types:

**Recursive models**

Such models are systems of equations that do not admit reciprocal effects or feedback loops. In that case, it is possible to write $\mathbf{B}$ as a lower triangular matrix, and the covariance matrix of the errors in the equations ($\boldsymbol{\Psi}$) is diagonal [15], which means that the disturbances for one equation are uncorrelated with the disturbances of the other equations. Recursive models are always identified.

**Nonrecursive models**

These contain reciprocal effects, feedback loops, or they have correlated disturbances [3]. In this case, $\mathbf{B}$ is not lower triangular, or the $\boldsymbol{\Psi}$ matrix is not diagonal. Given the excess of parameters in nonrecursive models, they can easily be unidentified.

## 3.2 Implied covariance matrix and correlation structures

The fundamental hypothesis for SEM is that the covariance matrix of the observed variables is a function of a set of parameters, i.e.

$$\boldsymbol{\Sigma} = \boldsymbol{\Sigma}(\boldsymbol{\theta}) \tag{3.2}$$

where $\boldsymbol{\Sigma}$ is the population covariance matrix of $\mathbf{x}$ and $\mathbf{y}$, $\boldsymbol{\theta}$ is a vector of model parameters, and $\boldsymbol{\Sigma}(\boldsymbol{\theta})$ is the covariance matrix written as a function of the free model parameters in $\boldsymbol{\theta}$. That implies that each element of the covariance matrix is a function of one or more model parameters. Therefore, if the model was correct, and if we knew the parameters, the population matrix would be exactly reproduced [3].

It is assumed that $\boldsymbol{\Sigma}$ is positive definite at every point $\theta_i$ of the admissible parameter space [22].

Alternatively, the covariance structure can also be expressed in terms of correlation matrix as

$$\boldsymbol{\Sigma} = \boldsymbol{D_\sigma P D_\sigma} \tag{3.3}$$

where $\boldsymbol{D_\sigma}$ is a diagonal matrix of population standard deviations $\sigma_1, \sigma_2, \cdots, \sigma_{m+n}$ for the $m+n$ variables under study.

The covariance matrix (3.2) can be partitioned into

$$\boldsymbol{\Sigma}(\boldsymbol{\theta}) = \begin{bmatrix} E(\mathbf{yy}') & E(\mathbf{yx}') \\ E(\mathbf{xy}') & E(\mathbf{xx}') \end{bmatrix} = \begin{bmatrix} (\mathbf{I}-\mathbf{B})^{-1}(\boldsymbol{\Gamma\Phi\Gamma}' + \boldsymbol{\Psi})(\mathbf{I}-\mathbf{B})^{-1'} & (\mathbf{I}-\mathbf{B})^{-1}\boldsymbol{\Gamma\Phi} \\ \boldsymbol{\Phi\Gamma}'(\mathbf{I}-\mathbf{B})^{-1'} & \boldsymbol{\Phi} \end{bmatrix} \tag{3.4}$$

Where $\boldsymbol{\Phi} = E(xx')$, or the covariance matrix of the exogenous variables $\mathbf{x}$, and $\boldsymbol{\Psi} = E(\boldsymbol{\zeta\zeta}')$, or the covariance matrix of the errors in the equations.

In the context of connectivity analysis, SEM are applied to the study of spontaneous activity within a neural network, rather than external inputs to said network [39]. As a result of this, there are no exogenous variables in the case of fMRI connectivity studies,

SEM model (3.1) is reduced to a path model and can be expressed as

$$\boldsymbol{y} = \boldsymbol{B}\boldsymbol{y} + \boldsymbol{\zeta} \tag{3.5}$$

while the covariance matrix (3.4) can be expressed as

$$\boldsymbol{\Sigma}(\boldsymbol{\theta}) = E(\mathbf{y}\mathbf{y}') = (\mathbf{I} - \mathbf{B})^{-1}\boldsymbol{\Psi}(\mathbf{I} - \mathbf{B})^{-1'} \tag{3.6}$$

Once a model has been specified, the variances and covariances are expressed as functions of the model parameters and can estimated.

## 3.3 Statistical assumptions underlying Structural Equation Modelling

As any parametric statistical technique, SEM requires that some underlying assumptions be satisfied in order to obtain accurate inferences.

Firstly, it is implied that the observations are drawn from a continuous multivariate normal population. If this condition is not satisfied, standard errors can be underestimated, while the likelihood ratio chi-square statistic can be severely overestimated [24].

Secondly, it is assumed that the observations are complete in all variables in the model. Several approaches have been developed in order to deal with missing data, but due to the characteristics of the current study, this will not be a concern.

Finally, SEM supposes that there is no specification error, or omission of relevant variables in any equation of the system of equations defined by the model. Specification errors would induce a correlation between errors and exogenous variables.

## 3.4 Identification

Identification of a model consists on evaluating whether it is theoretically possible to derive a unique set of model parameter estimates [26]. The researcher must establish whether unique values exist for those parameters whose identification status is not

known. Thus, identification is proved by showing that the unknown parameters are functions only of the identified parameters and that these functions lead to unique solutions [3].

The estimation methods will lead to consistent estimations for those parameters that are identified. If a model is not identified, it is possible to impose restrictions on the parameters. However, the choice of the restriction may affect the interpretation of the results [22].

In general terms, being $\boldsymbol{\theta}$ the sample space that generates a matrix $\boldsymbol{\Sigma}$, a model is identified whenever two different sample spaces $\boldsymbol{\theta}_i$ and $\boldsymbol{\theta}_j$ produce the same $\boldsymbol{\Sigma}$, and then the estimations do not have a unique solution [15]. In short, a model is identified if, and only if

$$\boldsymbol{\theta}_i \neq \boldsymbol{\theta}_j \Leftrightarrow \boldsymbol{\Sigma}(\boldsymbol{\theta}_i) \neq \boldsymbol{\Sigma}(\boldsymbol{\theta}_j) \tag{3.7}$$

Given that the equations we use to estimate the parameters come from the decomposition of the matrices $\boldsymbol{\Sigma}$ or $\mathbf{P}$, being $t$ the number of parameters to estimate and being $k = n+m$ the number of variables in the model, it will be identified if

$$t \leq \frac{1}{2}k(k+1) \tag{3.8}$$

where the right side of the inequality are the number of equations in the system. If the model is not identified, then restrictions can be imposed to $\boldsymbol{\theta}$.

## 3.5 Estimation procedures

Once the model is identified, the model parameters $\boldsymbol{\theta}$ will be estimated using a discrepancy function $F(\mathbf{S}, \boldsymbol{\Sigma}(\boldsymbol{\theta}))$, where $\mathbf{S}$ is the sample covariance matrix, that must fulfil the following properties [3, 15]:

$$F(\mathbf{S}, \boldsymbol{\Sigma}(\boldsymbol{\theta})) \textit{ is a scalar} \tag{3.9}$$

$$F(\mathbf{S}, \boldsymbol{\Sigma}(\boldsymbol{\theta})) \geq 0 \tag{3.10}$$

$$F(\mathbf{S}, \boldsymbol{\Sigma}(\boldsymbol{\theta})) = 0 \quad iff \quad \mathbf{S} = \boldsymbol{\Sigma}(\boldsymbol{\theta}) \tag{3.11}$$

$$F(\mathbf{S}, \boldsymbol{\Sigma}(\boldsymbol{\theta})) \textit{ is continuous in } \mathbf{S} \textit{ and } \boldsymbol{\Sigma}(\boldsymbol{\theta}) \tag{3.12}$$

The most widely used discrepancy functions are either Least Squares based methods such as Ordinary, Weighted, and Generalized Least Squares, or the Maximum Likelihood (ML) based methods. In the current case, the latter will be used.

Maximum Likelihood method minimizes

$$F_{ML} = \log|\boldsymbol{\Sigma}(\boldsymbol{\theta})| + tr(\mathbf{S}\boldsymbol{\Sigma}^{-1}(\boldsymbol{\theta})) - \log|\mathbf{S}| - (p+q) \tag{3.13}$$

This estimation method assumes that observations must follow a multivariate normal distribution, while $\mathbf{S}$ must follow a Wishart distribution and be positively defined with $n-1$ degrees of freedom.

## 3.6 Model evaluation

Once the model parameters have been estimated, it is key to assess the degree to which the model is able to accurately reproduce the observed data, and this is evaluated by means of fit indexes. Modern SEM software provides a wide variety of fit statistics, still we will highlight four of the most frequently used fit indexes [26]. The first of them is the model chi-square, while the remaining three a part of a generation of approximative fit indexes.

**Likelihood ratio chi-square**

Also known as *generalized likelihood ratio*, is the product of $(N-1)F_{ML}$, where $N$ is the sample size. Assuming multivariate normality, it follows a chi-square distribution with the degrees of freedom of the model $df_M$. This statistics tests

the overall fit, with the null hypothesis that there exists no discrepancies between the observed covariance matrix and the one predicted by the model.

It should be kept in mind that the observed value of the likelihood ratio chi-square, $\chi^2_M$, can be affected by several factors:

- Multivariate non-normality can greatly distort results
- Large correlations between observed variables lead to higher values of $\chi^2_M$
- Variables with high proportions of unique variance
- Sample size, so that very large samples can easily lead to rejection of null hypothesis

**Tucker-Lewis Index (TFI)**

This index estimates the proportion of covariances in the sample matrix explained by the model, and is expressed as

$$TLI = \frac{\frac{\chi^2_B}{df_B} - \frac{\chi^2_M}{df_M}}{\frac{\chi^2_B}{df_B} - 1} \tag{3.14}$$

where $\chi^2_B$ and $df_B$ refer to the $\chi^2$ and degrees of freedom of the baseline model, whereas $\chi^2_M$ and $df_M$ refer to the $\chi^2$ and degrees of freedom of the proposed model. While most values fall into $(0-1)$ range, values higher than 1 can be found in identified models or models with extremely low $\chi^2_M$, whereas values lower than 0 can be found in small samples or models with very poor fit. This index is particularly useful because it compensates for the complexity of the model [18].

**Comparative Fit Index (CFI)**

This index measures the relative improvement in the fit of the proposed model compared with a baseline model (denoted with the sub–index B), usually the null model with zero covariances between variables [1]. It is expressed as

$$CFI = 1 - \frac{\chi^2_M - df_M}{\chi^2_B - df_B} \tag{3.15}$$

This model has been often criticised because in several applications the null model may not be accepted as plausible.

**Root Mean Square Error of Approximation (RMSEA)**

This index follows a non-central chi-square distribution where the non-centrality parameter allows for discrepancies between model-implied and sample covariances up to the level of the expected value of $\chi^2_M$ [26, 42]. The RMSEA index is expressed as

$$RMSEA = \sqrt{\frac{\chi^2_M - df_M}{df_M(N-1)}} \tag{3.16}$$

Note that it is scaled inversely to the previously stated indexes, and values close to zero indicate the best fit.

## 3.7 Special considerations for its application to fMRI

Modelling brain connectivity by means of Path Analysis has limitations that must be taken into account. First, SEM does not permit the inclusion of the effect that a ROI might have on itself, which is particularly troublesome as data are in fact time series. In addition to this, non-recursive models constitute a more reasonable approach to functional connectivity than recursive models, allowing complex networks, yet they are usually more difficult to estimate.

Moreover, some statistical questions arise regarding biases that ROI selection may generate, and how it can affect the parameter estimation. In that regard, there is evidence that the number of brain volumes involved in the analysis and on the number of ROIs selected might bias the estimation of correlation between ROI values [6].

# Chapter 4

# Method

This chapter explains the participant selection procedure, as well as the technical details of fMRI scanning sessions and the experimental protocol.

## 4.1 Participants

The sample for this experiment consisted of 24 individuals (age $M = 21.83$ years, $SD = 5.02$, 10 women) from Guadalajara (Mexico) who where recruited for a previous study [17]. All participants were native Spanish speakers, with either normal or corrected eyesight, right-handed (according to the Edinburgh handedness inventory [35]), and none of them presented a history of neurological illness or learning disorders that could hinder their performance in the tasks. Informed consent was requested before the experiment and all participants recieved an economic compensation.

In a preliminary stage of the study, the command of homophone spelling in Spanish language (for instance, differentiating b *vs.* v, c-s-z, g *vs.* j, ll *vs.* y, or h *vs.* no h) of 827 individuals was assessed through four different tasks:

- Word completion
- Dictation of both words and text
- Error detection in a text
- Free composition

This assessment was executed by experimented researchers and its results were used to discriminate the participants according to their performance. This method showed an adequate reliability (Cronbach's $\alpha = 0.833$) and a very high discrimination capacity that allowed to distinguish between groups with different orthographic skills ($t = 11.608$, $p < 0.001$).

Out of these 827 participants, twelve individuals below 10th percentile in the tasks scores were selected and paired with twelve other participants above 90th percentile . Thus, the first group of people were considered to have low spelling skills (LSS group, hereafter), whereas the second group were assumed to have high spelling skills (HSS group, henceforth).

The resulting 24 individuals composed the sample for the brain connectivity experiment.

## 4.2 Instrument details

Image acquisition was conducted by the same research group though a GE Signa Excite HDxTde (GE Medical Systems, Milwaukee, WI) of 1.5 Teslas and 8 channel head coil.

For each experimental task, 32 adjacent axial cuts of 4 millimetres of thickness were obtained. An echo planar pulse sequence was used with a repetition time of 3 seconds, echo time of 60 milliseconds, 26 cm. Field of View, and a $64 \times 64$ matrix. Therefore, the voxel size in this study was $4.06 \times 4.06 \times 4$ mm.

Finally, a total of 62 brain volumes were obtained for each task. However, due to the image acquisition process, six volumes per task were discarded. Therefore, 56 brain volumes per task were used in the statistical analysis. Image pre-processing was conducted with SPM8 suit for MATLAB [17], through which images were religned spatially, readjusted to the voxel size, and normalized according to the Montreal Neurological Institute (MNI, hereafter) and Talairach coordinates.

A Kernel Gaussian filter three times the voxel size was used for smoothing, and Regions of Interest (ROI) were formed through the MarsBar software. Table 4.1 shows the $(x, y, z)$ MNI coordinates for each ROI in each task of this study.

| ROI | Anatomical Region | MNI coordinates | | |
|---|---|---|---|---|
| | | $x$ | $y$ | $z$ |
| *Spelling recognition task* | | | | |
| 1 | Right Precentral Gyrus (RPCG) | (64,68) | (-6,10) | (10,30) |
| 2 | Left Inferior Temporal Gyrus (LITG) | (64,-50) | (-32,-50) | (0,-18) |
| 3 | Right Middle Temporal Gyrus (RMTG) | (52,70) | (15,-41) | (-2,-22) |
| 4 | Left Cerebellum, Posterior Lobule (LCPL) | (-42,-22) | (-46,-36) | (-38,-30) |
| 5 | Left Middle Frontal Gyrus (LMFG) | (-50,-22) | (-10,10) | (42,58) |
| 6 | Right Supramarginal Gyrus (RSMG) | (48,62) | (-60,-44) | (26,36) |
| 7 | Left-Right Anterior Cingulate (LRAC) | (-4,6) | (30,38) | (-10,14) |
| 8 | Left Parahippocampal Gyrus (LPHG) | (-24,-14) | (-18,6) | (-22,-14) |
| *Visuoperceptual recognition task* | | | | |
| 1 | Right Precentral Gyurs (RPCG) | (52,86) | (-18,10) | (2,26) |
| 2 | Left-Right Middle Frontal Gyrus (LRMFG) | (-16,24) | (-26,2) | (46,74) |
| 3 | Left Middle Frontal Gyrus (LMFG) | (-50,-34) | (6,18) | (30,54) |
| 4 | Left Precentral Gyrus 1 (LPCG1) | (-66,-58) | (-18,2) | (-6,14) |
| 5 | Right Superior Frontal Gyrus (RSFG) | (4,16) | (50,56) | (22,34) |
| 6 | Left Precentral Gyrus 2 (LPCG2) | (-46,-26) | (-14,-26) | (52,70) |

TABLE 4.1: MNI coordinates $(x, y, z)$ of each ROI in each experimental task (Table adapted from Guàrdia-Olmos, et al. (2014b)[17])

## 4.3 Experimental procedure

The experiment comprised two different tasks in a block design: *spelling recognition* (A-B blocks) and *visuoperceptual recognition* (C-D blocks). In the spelling recognition task, participants were asked to make a quick decision on whether the word presented as stimulus was spelled correctly or not. Likewise, in the visuoperceptual recognition task, they were asked to decide whether the word presented contained a "i" or not regardless of the spelling. The participants response was submitted through two buttons, one for each response modality.

Participants were exposed to a total of 80 Spanish words, 20 of which contained a homophone orthographic error. For instance, *sapato* instead of the correct form *zapato*, which is the Spanish word for "shoe".

The stimuli were presented in Arial 60 font, typed in white on a black background, and were presented randomly during one second. There was a one second interval between stimuli. Half of the words were presented in A-B blocks, and the other half in C-D blocks.

In each task, four resting blocks were presented where the participants were not supposed to conduct any activity. In these blocks a centre fixation dot was shown. The change of the colour in the fixation dot warned the participants of the beginning of the block.

In like manner, four activation blocks were presented with ten stimuli in each block. Two of the blocks contained 50% of the words spelled incorrectly, whereas the other two blocks only included correctly spelled words.

## 4.4 Modelling procedure

Modelling procedure was executed as recommended by Inman, James et al. [20], constructing the linear equations of SEM describing the relations between ROI BOLD time courses.

Once all ROIs in each task had been identified, an initial saturated model was declared for each group in order to model the covariance matrices, and path coefficients were estimated using Mplus software [34]. All models that did not converge were excluded, as well as those with GFI or TLI lower than 0.1 or no significant paths.

For each group and task the best model was selected, with the lowest RMSEA, Akaike information criterion (AIC) and Bayesian information criterion (BIC).

# Chapter 5

# Results

The first part of this chapter will present the descriptive statistics for each experimental task. Immediately after, the models results will be displayed for each task and group. Given that all observations were complete, no missing data treatment was required.

## 5.1 Descriptive analysis

### 5.1.1 Spelling recognition task (A-B blocks)

Table 5.2 presents for each group the descriptive statistics of activation in the eight ROIs involved in the spelling recognition task (A-B blocks), and makes evident a considerably higher dispersion among the LSS group, which is illustrated in Figure 5.1.

Related to normality assessment, it was testified in both groups through Shapiro-Wilk Multivariate Normality Test that neither original data, nor its logarithmic transformations, fitted a multivariate distribution 5.1.

| Group | Data | W | p-value |
|---|---|---|---|
| HSS | Original | 0.914 | $< 0.001$ |
| | LT | 0.964 | $< 0.001$ |
| LSS | Original | 0.821 | $< 0.001$ |
| | LT | 0.819 | $< 0.001$ |

TABLE 5.1: Shapiro-Wilk Multivariate Normality Test, A-B blocks.
LT: logarithmic transformation

Univariate normality was also studied and it was resolved that data adjusted inadequately to a normal distribution, specially in LSS group. Table 5.3 displays the results of the Shapiro-Wilk normality test, and it can be verified that most contrasts were markedly significant, which is supported by Figures 5.2 and 5.3.

| Group | ROI | Mean (SD) | Min. | Max. | 1st Q | Median | 3rd Q |
|---|---|---|---|---|---|---|---|
| HSS | 1 | 131.90 (0.27) | 131.30 | 132.40 | 131.74 | 131.92 | 132.09 |
| | 2 | 99.63 (0.22) | 99.28 | 100.11 | 99.47 | 99.65 | 99.80 |
| | 3 | 137.17 (0.30) | 136.57 | 137.66 | 136.92 | 137.20 | 137.41 |
| | 4 | 181.99 (0.32) | 181.08 | 182.63 | 181.81 | 182.00 | 182.16 |
| | 5 | 153.04 (0.25) | 152.38 | 153.38 | 152.93 | 153.13 | 153.20 |
| | 6 | 104.33 (0.20) | 103.94 | 104.66 | 104.18 | 104.30 | 104.50 |
| | 7 | 152.72 (0.34) | 152.32 | 153.27 | 152.45 | 152.58 | 153.12 |
| | 8 | 104.23 (0.18) | 103.94 | 104.62 | 104.11 | 104.18 | 104.38 |
| LSS | 1 | 134.88 (9.40) | 113.47 | 149.55 | 127.32 | 137.50 | 141.98 |
| | 2 | 105.76 (8.48) | 92.62 | 123.22 | 98.92 | 105.36 | 112.26 |
| | 3 | 138.25 (7.11) | 122.96 | 151.70 | 137.05 | 138.47 | 141.97 |
| | 4 | 181.93 (8.80) | 166.33 | 199.83 | 177.27 | 182.71 | 187.10 |
| | 5 | 155.46 (11.29) | 143.55 | 181.54 | 146.44 | 152.51 | 162.20 |
| | 6 | 103.93 (3.25) | 98.05 | 109.93 | 100.88 | 105.00 | 106.08 |
| | 7 | 150.67 (4.29) | 147.96 | 165.89 | 148.66 | 149.05 | 149.75 |
| | 8 | 101.54 (1.69) | 100.48 | 107.57 | 100.73 | 100.92 | 101.15 |

TABLE 5.2: Descriptive statistics of the A-B blocks

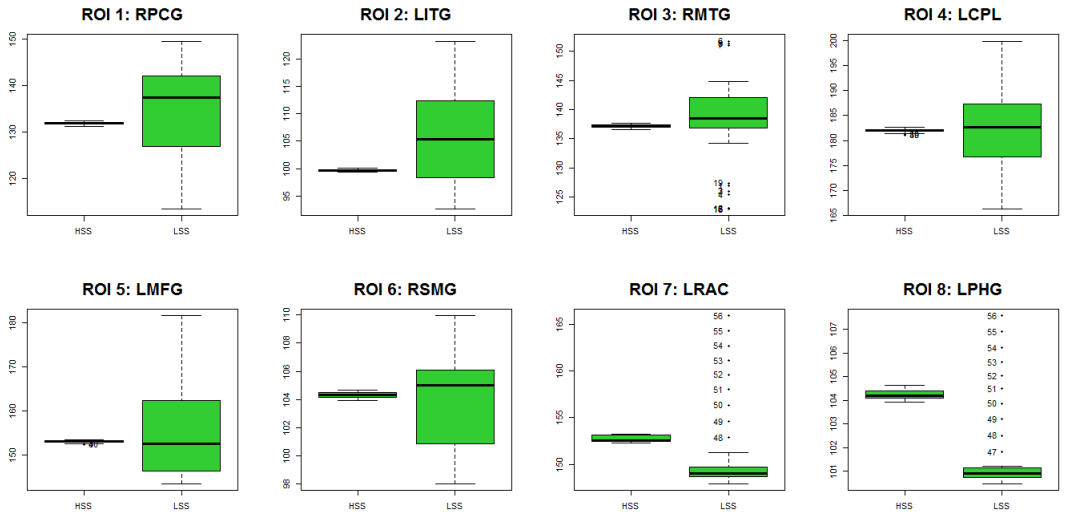


FIGURE 5.1: ROI activation of HSS and LSS in AB

As a second step, correlation matrices were obtained. As shown in table 5.4, moderate to high positive and negative correlations were observed between ROIs in HSS groups, while most correlations were notably lower in intensity in LSS group. It must be highlight

| Group | ROI | W | p-value |
|---|---|---|---|
| HSS | 1 | 0.965 | 0.102 |
| | 2 | 0.964 | 0.090 |
| | 3 | 0.962 | 0.077 |
| | 4 | 0.968 | 0.149 |
| | 5 | 0.904 | $< 0.001$ |
| | 6 | 0.951 | 0.024 |
| | 7 | 0.835 | $< 0.000$ |
| | 8 | 0.943 | 0.011 |
| LSS | 1 | 0.937 | 0.006 |
| | 2 | 0.942 | 0.009 |
| | 3 | 0.902 | $< 0.001$ |
| | 4 | 0.960 | 0.060 |
| | 5 | 0.861 | $< 0.001$ |
| | 6 | 0.939 | 0.007 |
| | 7 | 0.585 | $< 0.001$ |
| | 8 | 0.579 | $< 0.001$ |

TABLE 5.3: Shapiro-Wilk normality test in AB blocs

that the correlation between $ROI_7$ and $ROI_8$ was almost perfect in both groups, which alerts of collinearity problems.

| Group | ROIs | 1 | 2 | 3 | 4 | 5 | 6 | 7 |
|---|---|---|---|---|---|---|---|---|
| HSS | 2 | -0.186 | | | | | | |
| | 3 | 0.408 | 0.413 | | | | | |
| | 4 | 0.357 | 0.102 | -0.224 | | | | |
| | 5 | 0.523 | 0.289 | 0.423 | 0.447 | | | |
| | 6 | 0.132 | 0.750 | 0.792 | -0.065 | 0.480 | | |
| | 7 | -0.561 | 0.575 | -0.081 | 0.075 | -0.195 | 0.305 | |
| | 8 | -0.588 | 0.511 | -0.109 | 0.014 | -0.253 | 0.255 | 0.969 |
| LSS | 2 | 0.098 | | | | | | |
| | 3 | -0.064 | 0.418 | | | | | |
| | 4 | 0.617 | -0.368 | -0.127 | | | | |
| | 5 | -0.029 | 0.233 | 0.506 | -0.125 | | | |
| | 6 | 0.144 | -0.026 | 0.519 | 0.267 | 0.429 | | |
| | 7 | -0.240 | -0.009 | 0.005 | -0.279 | 0.129 | 0.230 | |
| | 8 | -0.260 | -0.017 | 0.002 | -0.291 | 0.122 | 0.229 | 0.999 |

TABLE 5.4: Pearson's Correlations of the HSS and LSS groups, A-B blocks

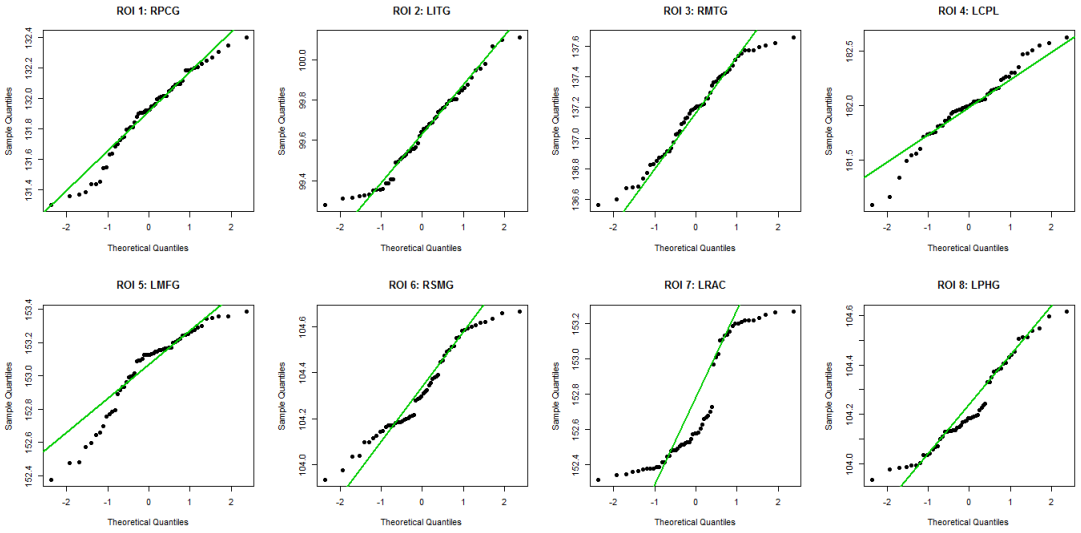


FIGURE 5.2: Q-Q plots of the HSS' ROI activation in A-B blocks.

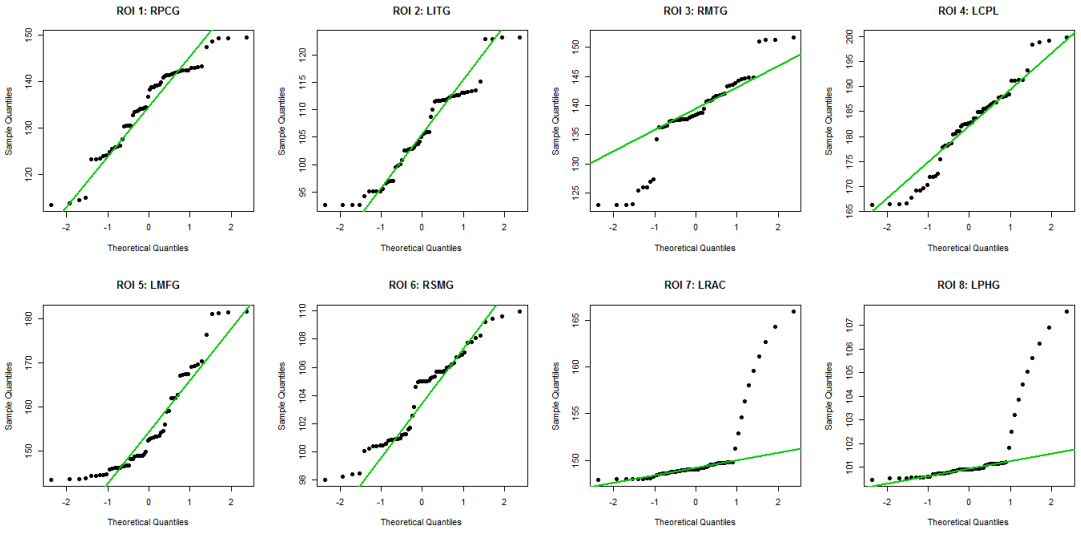


FIGURE 5.3: Q-Q plots of the LSS' ROI activation in A-B blocks.

### 5.1.2 Visuoperceptual recognition task (C-D blocks)

Related to the visuoperceptual recognition task, both groups presented low dispersion in activation values, with the HSS showing slightly higher activation in $ROI_1$ and $ROI_2$, and only just smaller activation values in $ROI_3$ to $ROI_5$, which can be seen in Table 5.5 and Figure 5.4.

| Group | ROI | Mean (SD) | Min. | Max. | 1st Q | Median | 3rd Q |
|---|---|---|---|---|---|---|---|
| HSS | 1 | 161.07 (0.31) | 160.38 | 161.86 | 160.83 | 161.08 | 161.24 |
| | 2 | 147.61 (0.27) | 147.18 | 148.42 | 147.40 | 147.58 | 147.73 |
| | 3 | 128.91 (0.30) | 128.22 | 129.57 | 128.71 | 128.85 | 129.14 |
| | 4 | 114.73 (0.31) | 114.11 | 115.43 | 114.54 | 114.74 | 114.91 |
| | 5 | 171.04 (0.33) | 170.27 | 171.85 | 170.82 | 171.01 | 171.22 |
| | 6 | 127.79 (0.74) | 126.73 | 129.15 | 127.07 | 127.81 | 128.47 |
| LSS | 1 | 153.26 (0.23) | 152.83 | 153.99 | 153.12 | 153.27 | 153.38 |
| | 2 | 140.19 (0.24) | 139.61 | 140.83 | 140.01 | 140.20 | 140.33 |
| | 3 | 133.11 (0.36) | 132.49 | 134.14 | 132.86 | 133.05 | 133.37 |
| | 4 | 119.36 (0.21) | 118.94 | 119.98 | 119.22 | 119.36 | 119.47 |
| | 5 | 174.17 (0.40) | 173.27 | 175.02 | 173.83 | 174.21 | 174.47 |
| | 6 | 126.14 (0.66) | 124.89 | 127.09 | 125.51 | 126.19 | 126.73 |

TABLE 5.5: Descriptive statistics of C-D blocks

From multivariate normality assessment it was concluded that data from none of the groups adjusted to a multivariate normal distribution (Table 5.6). Nonetheless, most variables adjusted well to a normal distribution as it is shown in Table 5.7 and Figures 5.5 and 5.6, with the exceptions of $ROI_6$ both groups, and in a lesser extend $ROI_2$ in group HSS.

| Group | Data | W | p-value |
|---|---|---|---|
| HSS | Original | 0.932 | $< 0.004$ |
| | LT | 0.932 | $< 0.004$ |
| LSS | Original | 0.877 | $< 0.001$ |
| | LT | 0.878 | $< 0.001$ |

TABLE 5.6: Shapiro-Wilk Multivariate Normality Test, C-D blocks.
LT: logarithmic transformation

Regarding the degree of association between ROIs in the visuoperceptual task, all Pearson's correlations coefficients were positive with a moderate to high intensity, as it is displayed in Table 5.8).

| Group | ROI | W | p-value |
|---|---|---|---|
| HSS | 1 | 0.991 | 0.951 |
| | 2 | 0.956 | 0.042 |
| | 3 | 0.975 | 0.285 |
| | 4 | 0.986 | 0.761 |
| | 5 | 0.984 | 0.675 |
| | 6 | 0.903 | $< 0.001$ |
| LSS | 1 | 0.978 | 0.398 |
| | 2 | 0.989 | 0.898 |
| | 3 | 0.979 | 0.421 |
| | 4 | 0.961 | 0.066 |
| | 5 | 0.985 | 0.703 |
| | 6 | 0.920 | 0.001 |

TABLE 5.7: Shapiro-Wilk normality test in C-D blocs

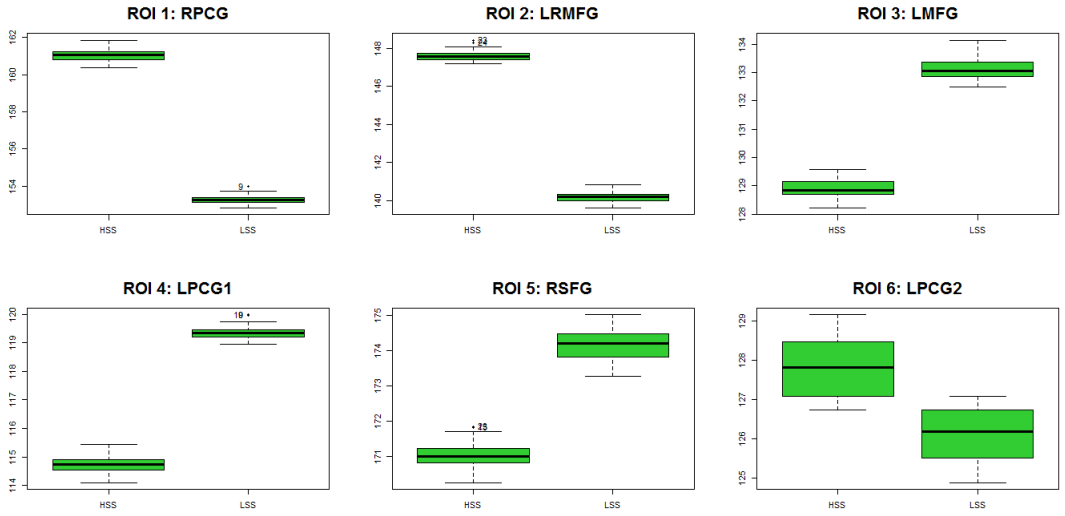


FIGURE 5.4: ROI activation of the HSS and LSS' in CD.

| Group | ROIs | 1 | 2 | 3 | 4 | 5 |
|---|---|---|---|---|---|---|
| HSS | 2 | 0.708 | | | | |
| | 3 | 0.203 | 0.470 | | | |
| | 4 | 0.945 | 0.685 | 0.285 | | |
| | 5 | 0.035 | 0.236 | 0.704 | 0.042 | |
| | 6 | 0.435 | 0.736 | 0.484 | 0.529 | 0.025 |
| LSS | 2 | 0.691 | | | | |
| | 3 | 0.259 | 0.755 | | | |
| | 4 | 0.811 | 0.707 | 0.412 | | |
| | 5 | 0.588 | 0.574 | 0.473 | 0.352 | |
| | 6 | 0.160 | 0.591 | 0.688 | 0.501 | -0.145 |

TABLE 5.8: Pearson's Correlations of the HSS and LSS groups, C-D blocks

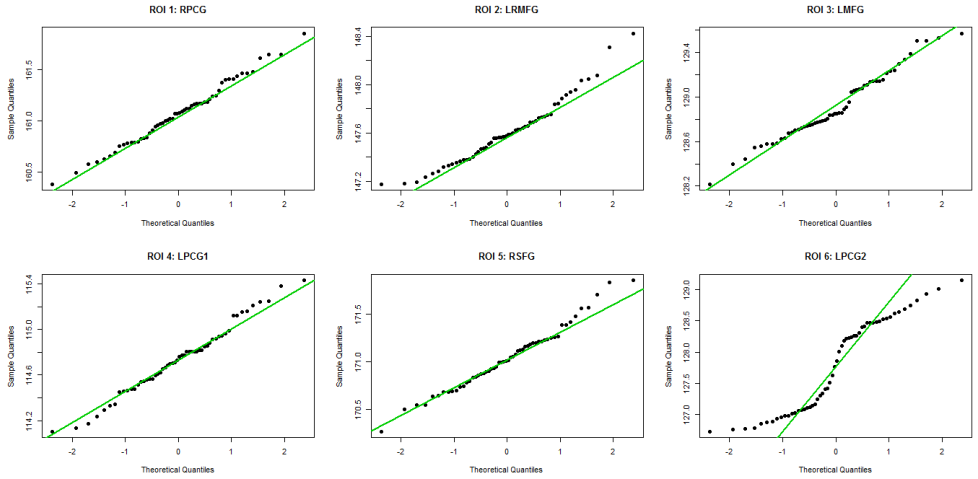


FIGURE 5.5: Q-Q plots of the HSS' ROI activation in CD.

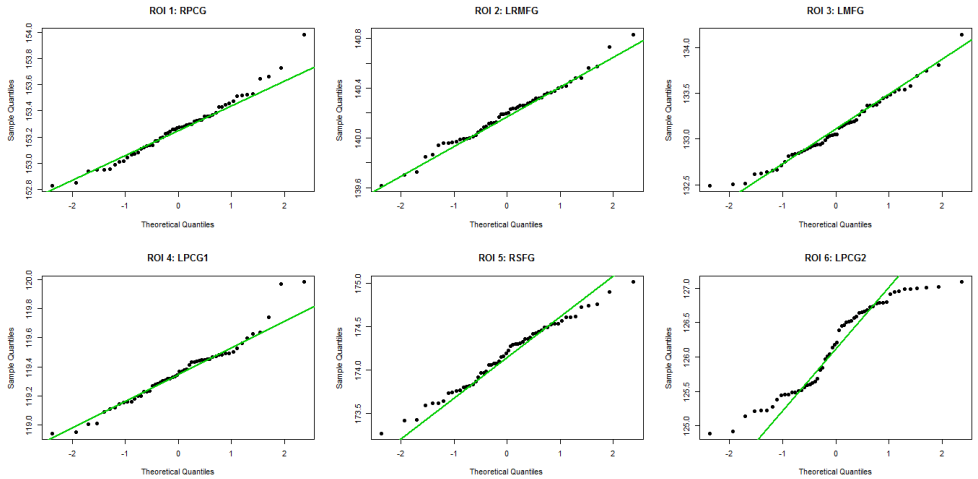


FIGURE 5.6: Q-Q plots of the LSS' ROI activation in CD.

## 5.2 Structural Equation Modelling

Table 5.9 displays the model fit indexes of the best models obtained for each condition. As it can be seen, all $\chi^2$ statistics were significant, except for that of the LSS group in the visuoperceptual recognition task (C-D blocks).

Related to CFI and TLI considered together in the models for HSS in each experimental condition, their values fail to consistently surpass the usual cut-off threshold of 0.95 [18]. Similarly, RMSEA values fail to fall below the threshold of 0.06 [18]. Therefore, even though those were selected as the best models for each task, it can be concluded that these models present a poor fit.

| | **A-B blocks** | | **C-D blocks** | |
|---|---|---|---|---|
| | HSS | LSS | HSS | LSS |
| $\chi^2$ | 21.762 | 161800.708 | 19.652 | 2.598 |
| d.f. | 8 | 9 | 6 | 4 |
| p-value | 0.005 | $< 0.001$ | 0.003 | 0.627 |
| CFI | 0.952 | $< 0.001$ | 0.938 | 1.000 |
| TLI | 0.899 | -780.005 | 0.897 | 1.015 |
| AIC | -316.874 | 474316.990 | -0.477 | -119.103 |
| BIC | -248.012 | 474343.320 | 38.005 | -72.520 |
| RMSEA | 0.175 | - | 0.202 | 0.000 |

TABLE 5.9: Best models for each task and group

The model for LSS group in the spelling recognition task (C-D blocks) deserves special attention. This was the only model that reached convergence, however no modifications allowed to improve the fit. In this case, $\chi^2$ statistics was significant, both CFI and TLI were notably low, whereas and AIC and BIC were exceedingly high. Additionally, RMSEA index could not defined.

Finally, the best model for LSS group in the visuoperceotual task (C-D blocks), showed a specially good fit according to the previously stated criteria, yet that was at the expense of the degrees of freedom.

### 5.2.1 Spelling recognition task (A-B block)

The model coefficients for the HSS group in the spelling recognition task are reported in Table 5.10. Following the Mplus language, the statement *ON* denotes a regression of a

variable $y$ on a variable $x$ and defines a directional path, whereas the statement *WITH* denotes a covariance relationship between two variables. Finally, "Res. Var." indicates those variables whose residual variances were freed for estimation.

Results suggest a complex network between all eight ROIs, with a few non significant paths that were kept in the model for fitting purposes. The strongest paths found in this network were the one from $ROI_7$ (LRAC) to $ROI_2$ in a positive trend, and from $ROI_8$ (LPHG) to $ROI_2$ (LITG) in a negative direction.

In addition to this, three covariance relationships were detected between $ROI_3$ (RMTG) and $ROI_1$ (RPCG), $ROI_4$ (LCPL) and $ROI_5$ (LMFG), as well as between $ROI_6$ and $ROI_3$ (RSMG).

TABLE 5.10: Best model for HSS group in A-B blocks

| | | Estimate | S.E. | IC(95%) | p-value |
|---|---|---|---|---|---|
| ROI1 on | 2 | 0.933 | 0.710 | (-0.459, 2.324) | 0.189 |
| | 3 | 4.013 | 0.625 | (2.789, 5.237) | $< 0.001$ |
| | 4 | 4.721 | 0.785 | (3.183, 6.259) | $< 0.001$ |
| | 5 | -5.678 | 0.788 | (0.059, -4.134) | $< 0.001$ |
| | 7 | -2.447 | 0.895 | (-4.201, -0.692) | 0.006 |
| ROI2 on | 1 | 2.977 | 0.819 | (1.371, 4.583) | $< 0.001$ |
| | 3 | -0.420 | 0.932 | (-2.246, 1.406) | 0.652 |
| | 4 | -1.863 | 0.726 | (-3.286, -0.441) | 0.010 |
| | 5 | -0.289 | 0.617 | (-1.498, 0.921) | 0.640 |
| | 7 | 18.136 | 2.125 | (13.971, 22.300) | $< 0.001$ |
| | 8 | -15.382 | 2.069 | (-19.438, -11.326) | $< 0.001$ |
| ROI3 on | 1 | -0.629 | 0.190 | (-1.001, -0.258) | 0.001 |
| | 2 | -3.784 | 0.612 | (-4.984, -2.584) | $< 0.001$ |
| | 4 | -2.590 | 0.430 | (-3.433, -1.748) | $< 0.001$ |
| | 5 | 3.557 | 0.418 | (2.738, 4.377) | $< 0.001$ |
| | 7 | 2.188 | 0.684 | (0.847, 3.529) | 0.001 |
| ROI4 on | 1 | -1.882 | 0.299 | (-2.467, -1.297) | $< 0.001$ |
| | 2 | 0.242 | 0.261 | (-0.269, 0.753) | 0.353 |

*Continued on next page*

Table 5.10 – *Continued from previous page*

| | | Estimate | S.E. | IC(95%) | p-value |
|---|---|---|---|---|---|
| | 3 | 1.554 | 0.490 | (0.594, 2.515) | 0.002 |
| ROI5 on | 1 | 3.236 | 0.414 | (2.424, 4.047) | $< 0.001$ |
| | 3 | -4.091 | 0.395 | (-4.865, 0.172) | $< 0.001$ |
| ROI6 on | 1 | -0.871 | 0.125 | (-1.116, -0.626) | $< 0.001$ |
| | 2 | -1.791 | 0.492 | (-2.755, -0.826) | $< 0.001$ |
| | 3 | 1.663 | 0.194 | (1.283, 2.043) | $< 0.001$ |
| | 7 | 0.575 | 0.410 | (-0.229, 1.379) | 0.161 |
| ROI7 on | 1 | 2.016 | 0.275 | (1.478, 2.555) | $< 0.001$ |
| | 4 | -2.438 | 0.300 | (0.061, -1.849) | $< 0.001$ |
| ROI8 on | 1 | -0.634 | 0.061 | (-0.753, -0.515) | $< 0.001$ |
| | 5 | -0.065 | 0.080 | (-0.221, 0.091) | 0.417 |
| ROI3 with | 1 | -0.753 | 0.083 | (-0.916, -0.590) | $< 0.001$ |
| ROI5 with | 4 | -0.860 | 0.031 | (-0.920, -0.799) | $< 0.001$ |
| ROI6 with | 3 | 0.639 | 0.099 | (0.445, 0.833) | $< 0.001$ |
| Res. Var. | 6 | 2.668 | 1.082 | (0.546, 4.790) | 0.014 |
| | 8 | 0.340 | 0.038 | (0.265, 0.414) | $< 0.001$ |

Related to the model for LSS group in the spelling recognition task, the results are displayed in Table 5.11. However, given the inadequate fit, this results are in no condition to be interpreted.

TABLE 5.11: Best model for LSS group in A-B blocks

| | | Estimate | S.E. | IC(95%) | p-value |
|---|---|---|---|---|---|
| ROI1 on | 2 | 0.232 | 0.097 | (0.042, 0.421) | 0.017 |
| | 3 | -0.569 | 0.049 | (-0.665, -0.473) | $< 0.001$ |
| | 4 | 0.327 | 0.013 | (0.302, 0.352) | $< 0.001$ |
| | 6 | 0.273 | 0.020 | (0.235, 0.311) | $< 0.001$ |

*Continued on next page*

Table 5.11 – *Continued from previous page*

| | | Estimate | S.E. | IC(95%) | p-value |
|---|---|---|---|---|---|
| | 7 | -1.075 | 0.044 | (-1.162, -0.989) | $< 0.001$ |
| ROI2 on | 1 | -0.453 | 0.024 | (-0.500, -0.406) | $< 0.001$ |
| | 3 | 0.098 | 0.046 | (-0.475, -0.296) | $< 0.001$ |
| ROI3 on | 1 | -0.401 | 0.005 | (-0.410, -0.391) | $< 0.001$ |
| | 2 | -0.001 | 0.011 | (-0.024, 0.021) | 0.908 |
| ROI5 on | 1 | -0.467 | 0.003 | (-0.473, -0.461) | $< 0.001$ |
| ROI6 on | 1 | -0.498 | 0.003 | (-0.504, -0.492) | $< 0.001$ |
| ROI7 on | 1 | -0.408 | 0.002 | (-0.412, -0.404) | $< 0.001$ |
| ROI8 on | 1 | -0.486 | 0.002 | (-0.489, -0.483) | $< 0.001$ |

### 5.2.2 Visuoperceptual recognition task (C-D block)

Related to the model for HSS group in the visuoperceptual task, the strongest path coefficients were detected in $ROI_3$ (LMFG) through both $ROI_1$ (RPCG) and $ROI_4$ (LPCG1) whereas no covariance effects were revealed. Incidentally, some path coefficients were significant, in spite of being extremely low.

Table 5.12: Best model for HSS group in C-D blocks

| | | Estimate | S.E. | IC(95%) | p-value |
|---|---|---|---|---|---|
| ROI1 on | 2 | -2.776 | 0.537 | (-3.828, -1.723) | $< 0.001$ |
| | 3 | -2.748 | 0.682 | (-4.084, -1.411) | $< 0.001$ |
| | 5 | 3.037 | 0.505 | (2.047, 4.028) | $< 0.001$ |
| | 6 | 4.993 | 0.480 | (4.052, 5.934) | $< 0.001$ |
| ROI2 on | 1 | 0.655 | 0.342 | (-0.015, 1.325) | 0.055 |
| | 3 | -3.572 | 0.371 | (-4.299, -2.846) | $< 0.001$ |
| | 5 | 2.365 | 0.384 | (1.613, 3.118) | $< 0.001$ |
| ROI3 on | 1 | -12.950 | 1.658 | (-16.199, -9.700) | $< 0.001$ |

*Continued on next page*

Table 5.12 – *Continued from previous page*

| | | Estimate | S.E. | IC(95%) | p-value |
|---|---|---|---|---|---|
| | 2 | 4.518 | 0.909 | (2.737, 6.300) | $< 0.001$ |
| | 4 | 12.182 | 1.353 | (9.530, 14.833) | $< 0.001$ |
| | 6 | -3.329 | 0.721 | (-4.741, -1.916) | $< 0.001$ |
| ROI4 on | 1 | -1.637 | 0.574 | (-2.762, -0.512) | 0.004 |
| | 2 | 5.034 | 0.518 | (4.018, 6.050) | $< 0.001$ |
| | 3 | -3.358 | 0.286 | (-3.918, -2.797) | $< 0.001$ |
| ROI5 on | 2 | -0.847 | 0.062 | (-0.968, -0.725) | $< 0.001$ |
| | 3 | 0.677 | 0.079 | (0.522, 0.831) | $< 0.001$ |
| | 4 | 0.099 | 0.009 | (0.522, 0.118) | $< 0.001$ |
| | 6 | 0.251 | 0.024 | (0.203, 0.299) | $< 0.001$ |
| ROI6 on | 1 | -1.786 | 0.153 | (-2.086, -1.485) | $< 0.001$ |
| | 2 | 1.727 | 0.223 | (1.290, 2.164) | $< 0.001$ |
| | 3 | 0.037 | 0.003 | (0.031, 0.042) | $< 0.001$ |
| | 4 | 0.039 | 0.002 | (0.035, 0.044) | $< 0.001$ |
| | 5 | 0.040 | 0.004 | (0.032, 0.047) | $< 0.001$ |
| Res. Var. | 5 | 0.730 | 0.100 | (0.534, 0.926) | $< 0.001$ |

The model for LSS group in this task is no less complex than the rest of models presented, yet no covariances between ROIs were detected. With the exception of the paths from $ROI_4$ (LPCG1) and $ROI_6$ (LPCG2) to $ROI_1$ (RPCG), all coefficients were significantly different from zero, and the highest intensity connections were directed from $ROI_3$ (LMFG) and $ROI_5$ (RSFG) to $ROI_2$ (LRMFG).

Table 5.13: Best model for LSS group in C-D blocks

| | | Estimate | S.E. | IC(95%) | p-value |
|---|---|---|---|---|---|
| ROI1 on | 2 | 0.637 | 0.234 | (0.179, 1.095) | 0.006 |
| | 3 | -0.700 | 0.151 | (-0.996, -0.403) | $< 0.001$ |

*Continued on next page*

Table 5.13 – *Continued from previous page*

| | | Estimate | S.E. | IC(95%) | p-value |
|---|---|---|---|---|---|
| | 4 | -0.267 | 0.169 | (-0.598, 0.064) | 0.113 |
| | 6 | 0.184 | 0.166 | (-0.141, 0.508) | 0.267 |
| ROI2 on | 1 | -5.594 | 1.110 | (-7.770, -3.417) | $< 0.001$ |
| | 3 | -10.728 | 1.187 | (-13.054, -8.401) | $< 0.001$ |
| | 4 | 1.765 | 1.239 | (-0.663, 4.194) | 0.154 |
| | 5 | 10.628 | 1.262 | (8.155, 13.100) | $< 0.001$ |
| | 6 | 9.746 | 1.729 | (6.357, 13.135) | $< 0.001$ |
| ROI3 on | 1 | 5.398 | 0.796 | (3.837, 6.958) | $< 0.001$ |
| | 2 | -3.989 | 0.887 | (-5.727, -2.252) | $< 0.001$ |
| | 4 | -5.039 | 0.749 | (-6.506, -3.572) | $< 0.001$ |
| | 5 | 1.510 | 0.695 | (0.148, 2.872) | 0.030 |
| | 6 | 5.448 | 0.782 | (3.915, 6.980) | $< 0.001$ |
| ROI4 on | 2 | -5.854 | 0.628 | (-7.084, -4.623) | $< 0.001$ |
| | 3 | 5.703 | 0.815 | (4.106, 7.300) | $< 0.001$ |
| | 5 | 3.061 | 0.772 | (1.548, 4.575) | $< 0.001$ |
| ROI5 on | 2 | -4.073 | 0.573 | (-5.195, -2.950) | $< 0.001$ |
| | 3 | 1.997 | 0.698 | (0.629, 3.366) | 0.004 |
| | 4 | 2.829 | 0.510 | (1.828, 3.829) | $< 0.001$ |
| | 6 | 0.170 | 0.020 | (0.130, 0.210) | $< 0.001$ |
| ROI6 on | 1 | 0.819 | 0.228 | (0.372, 1.266) | $< 0.001$ |
| | 2 | -1.025 | 0.218 | (-1.453, -0.598) | $< 0.001$ |
| | 3 | 0.055 | 0.006 | (0.043, -0.598) | $< 0.001$ |
| | 4 | 0.031 | 0.003 | (0.025, 0.038) | $< 0.001$ |
| | 5 | 0.059 | 0.007 | (0.045, 0.073) | $< 0.001$ |
| Res. Var. | 1 | 1.006 | 0.079 | (0.850, 1.162) | $< 0.001$ |

On the whole it can be concluded that best models for each experimental condition and group obtained by means of structural equation models had difficulties to correctly fit the data, partially due to the complexity of the phenomenon, as well as the failure to satisfy the statistical assumptions.

# Chapter 6

# Discussion

The last few decades in Neuroscience have witnessed a steady growth of contributions that stressed that cognitive processes had to be understood as a complex interaction of segregated areas, rather than simply the disconnected activation of separated brain regions [11]. In order to do so, neuroscientists with diverse academic backgrounds have laid out several approaches to study how brain regions connect with each other when the individuals face a given cognitive task.

Among those approaches, functional connectivity studies what in statistical terms is the covariance over time among segregated brain regions that compound a functional network. This master's thesis has centred its focus on the use of the most extended tool to study ROI-based functional connectivity, Structural Equation Models.

While the estimation of brain connectivity with SEM does not take into consideration the biological architecture of the nervous system, it allows us to formulate stochastic structural relationships between ROIs that are activated in front a certain task.

In the current case, two different experimental conditions were applied to a group of individuals with good command of orthographic skills, and to a second group of individuals with low command. The first experimental procedure involved the detection of homophone orthographic mistakes in Spanish language in a sequence of written stimuli (spelling recognition), while the second experimental condition involved the detection of an "i" in the stimuli regardless of the spelling (visuoperceptual recognition). The latter is a classic example of a experiment on a cognitive interference effect.

In order to examine the functional connectivity in this setting, we have started, in each experimental condition and group, from a set of regions that had been obtained by a combination of both univariate and multivariate analyses of changes in signal intensity, which were consistent with the theoretical framework in neuroscience. The resulting ROI time series constituted our data.

At this point, SEM was used to fit a model for each group and condition and to estimate the path coefficients. It must be noted that, given the nature of the phenomenon under study, an inevitable complexity of the network must be considered. Therefore, although SEM does not allow to include the effect that a ROI can exert on itself, models with reciprocal effects and feedback loops should be regarded as a reasonable approach. The cost of such strategy is that this type of models are seldom easy to adjust [3, 15].

Among the limitations of this research it must be considered that the assumption of multivariate normality was not held in any of the conditions, in which case standard errors can be underestimated and the likelihood ratio $\chi^2$ statistic can be severely overestimated [24]. Moreover, the effects of non-normality were more severe in the case of LSS group in the spelling recognition task (A-B blocks).

In that same experiment an almost perfect correlation between $ROI_7$ and $ROI_8$ in both groups alerts of collinearity problems that remains unsolved, because combining the information on both areas would not be supported from a neurological standpoint.

And finally, related to the fact that SEM does not allow to consider the effects of a variable on itself is particularly worrisome since data points constitute a time series, and this information is ignored with SEM approaches.

All in all, we can conclude that given the nature of this phenomenon, the most feasible models are necessarily complex. Therefore, we should focus our attention to search for models that allow reciprocal influence between variables. Moreover, it essential to incorporate the effects that a ROI might exercise on itself, so as to reflect the change in intensity that are linked to time.

This work has permitted to identify certain issues in the application of SEM to functional connectivity research. As a result of which it would be interesting to study, by means of simulated BOLD signal, the impact of instrumental and methodological variables on the estimation of SEM. In that manner, we can study the viability of these models in the

field of brain connectivity, so that we can identify and propose a range of methodological directions to grant its proper use.

On the whole, with all its impediments, the study of brain connectivity constitutes this day the major challenge in the field of neuroscience, and it's by reaching better understanding of research methods, through the collaboration of different scientific disciplines, that ground for theoretic progress is set, which in turn will revert to finer work in clinical settings.

# Bibliography

[1] Bentler, P. M. (1990). Comparative fit indexes in structural models. *Psychological Bulletin*, 107:238–246.

[2] Bianchi, A., Marchetta, E., Tana, M., Tettamanti, M., and Rizzo, G. (2012). Frequency-based approach to the study of semantic brain networks connectivity. *Journal of Neuroscience Methods*, 212:181– 189.

[3] Bollen, K. A. (1989). *Structural Equations with Latent Variables*. Hoboken: John Wiley & Sons.

[4] Boynton, G. M., Engel, S. A., and Heeger, D. J. (2012). Linear systems analysis of the fmri brain signal. *NeuroImage*, 62:975–984.

[5] Buxton, R. B. (2002). *Introduction to Functional Magnetic Ressonance Imaging. Principles and techniques*. Cambridge: Cambridge University Press.

[6] Caclin, A. and Fonlupt, P. (2006). Effect of initial fmri data modelling on the connectivity reported between brain areas. *NeuroImage*, 33:515–521.

[7] Chen, G., Glen, D. R., Saad, Z. S., Hamilton, J. P., Thomason, M. E., Gotlib, I. H., and Cox, R. W. (2011). Vector autoregression, structural equation modeling, and their synthesis in neuroimaging data analysis. *Computers in Biology and Medicine*, 41:1142–1155.

[8] de Marco, D., Devauchelle, B., and Berquin, P. (2009a). Brain functional modelling, what do we measure with fMRI data. *Neuroscience Research*, 69:12–19.

[9] de Marco, D., Vrignaud, P., Destrieux, C., De Marco, D., Testelin, S., B., D., and Berquin, P. (2009b). Principle of structural equation modeling for exploring functional interactivity within a putative network of interconnected brain areas. *Magnetic Resonance Imaging*, 27:1–12.

[10] Friston, J. K., , Harrison, L., and Penny, W. (2003). Dynamic causal modelling. *NeuroImage*, 19:1273–1302.

[11] Friston, K. J. (2009). Modalities, model, and models in functional neuroimaging. *Science*, 309:399–403.

[12] Friston, K. J. (2011). Functional and effective connectivity: a review. *Brain Connectivity*, 1(1):13–36.

[13] Gates, K. M., Molenaar, P. C. M., Hillary, F. G., Ram, N., and Rovine, M. J. (2010a). Automatic search for fmri connectivity mapping: An alternative to granger causality testing using formal equivalences among sem path modeling, var, and unified sem. *NeuroImage*, 50:1118–1125.

[14] Gates, K. M., Molenaar, P. C. M., Hillary, F. G., and Slobounov, S. (2010b). Extended unified sem approach for modeling event-related fmri data. *NeuroImage*, 54:1151–1158.

[15] Guardia-Olmos, J. (1986). *Los sistemas de ecuaciones estructurales en el ámbito de la Psicología: análisis de un modelo de predicción de la ansiedad social.* Tesi Doctoral, Universitat de Barcelona, Barcelona.

[16] Guàrdia-Olmos, J., Peró-Cebollero, M., and Gudayol-Ferré, E. (2014a). Analysis of the use of structural equation models for the estimation of functional brain connectivity with fmri. *Cognitive Systems research*, Under editorial revision.

[17] Guàrdia-Olmos, J., Peró-Cebollero, M., Zarabozo-Hurtado, D., González-Garrido, A., and Gudayol-Ferré, E. (2014b). Functional and effective connectivity of visual word recognition and homophone orthographic errors. *Frontiers in Humane Neuroscience*, Under editorial revision.

[18] Hu, L. T. and Bentler, P. M. (1999). Cutoff criteria for fit indexes in covariance structure analysis. conventional criteria versus new alternatives. *Structural Equation Modeling. A Multidisciplinary Journal*, 6(1):1–55.

[19] Huettel, S. A., Song, A. W., and McCarthy, G. (2009). *Functional Magnetic Resonance Imaging.* Sunderland: Sinauer Associates.

[20] Inman, C. S., James, G. A., Hamann, S., Rajendra, J. K., P. G., and Butler, A. J. (2012). Altered resting-state effective connectivity of fronto-parietal motor control systems on the primary network following stroke. *NeuriImage*, 59:277–237.

[21] James, G. A., Kelley, M. E., Craddock, R. C., Holtzheimer, P. E., Dunlop, B. W., Nemeroff, C. B., Mayberg, H. S., and Hu, X. P. (2009). Exploratory structural equation modeling of resting-state fmri: Applicability of group models to individual subjects. *NeuroImage*, 45:778–787.

[22] Jöreskog, K. G. (1978). Structural analysis of covariance and correlation matrices. *Pychometrika*, 43(4):443–477.

[23] Junqué, C. and Barroso, J. (2009). *Manual de Neuropsicología*. Madrid: Síntesis.

[24] Kaplan, D. (2000). *Structural Equation Modeling. Foundations and Extensions*. Thousand Oaks: Sage.

[25] Kim, J. and Horwitz, B. (2009). How well does structural equation modeling reveal abnormal brain anatomical connections? an fmri simulation study. *NeuroImage*, 45:1190–1198.

[26] Kline, R. B. (2011). *Principles and Practice of Structural Equation Modeling*. New York: The Guildford Press.

[27] Lee, S. (1980). Estimation of covariance structure models with parameters subject to functional restrains. *Psychometrica*, 45(1):309–325.

[28] Li, K., Guo, L., Nie, J., Li, G., and Liu, T. (2009). Review of methods for brain functional connectivity detection using fMRI. *Computerized Medical Imaging and Graphics*, 33:131–139.

[29] Lindquist, M. A. (2008). The statistical analysis of fMRI data. *Statistical Science*, 23(4):439–464.

[30] McIntosh, A. and Gonzalez-Lima, F. (1991). Structural modeling of functional neural pathways mapped with 2-deoxyglucose: effects of acoustic startle habituation on the auditory system. *Brain Research*, 547:295–302.

[31] McIntosh, A. and Gonzalez-Lima, F. (1992). The application of structural modeling to metabolic mapping of functional neural systems. *Advances in Metabolic Mapping Techniques for Brain Imaging of Behavioral and Learning Functions*, 68:219–255.

[32] McIntosh, A. and Gonzalez-Lima, F. (1994). Structural equation modeling and its application to network analysis in functional brain imaging. *Human Brain Mapping*, 2:2–22.

[33] McIntosh, A. R. (1999). Mapping cognition to the brain through neural interactions. *Memory*, 7(5-6):523–548.

[34] Muthén, L. and Muthén, B. (1998-2007). *Mplus User's Guide. Fifth Edition.* Los Angeles: Muthén and Muthén.

[35] Oldfield, R. (1971). The assessment and analysis of handedness. The Edinburgh Inventory. *Neuropsychologia*, 9:97–113.

[36] Penke, L. and Deary, I. (2010). Some guidelines for structural equation modeling in cognitive neuroscience: The case of charlton et al.'s study on white matter integrity and cognitive ageing. *Neurobiology of Aging*, 31:1656–1660.

[37] Penny, W., Stephan, K., Mechelli, A., and Friston, K. (2004). Modelling functional integration: a comparison of structural equation and dynamic causal models. *NeuroImage*, 23:264–274.

[38] Redolar-Ripoll, D. (2014). *Neurociencia Cognitiva.* Madrid: Editorial Médica Panamericana.

[39] Rowe, J. B. (2010). Connectivity analysis is essential to understand neurological disorders. *Frontiers in Systems Neuroscience*, 4:1–13.

[40] Schlösser, R. G. M., Wagner, G., and Sauer, H. (2006). Assessing the working memory network: studies with functional magnetic resonance imaging and structural equation modeling. *Neuroscience*, 139:91–103.

[41] Smith, S. M. (2012). The future of brain connectivity. *NeuroImage*, 62:1257–1266.

[42] Steiger, J. H. (1990). Structural model evaluation and modification: An intervalestimation approach. *Multivariate Behavioural Research*, 25:173–180.

[43] Taylor, J., Krause, B., Shah, N., Horwitz, B., and Mueller-Gaertner, H. (2010). On the relation between brain images and brain neural networks. *Human Brain Mapping*, 9:165–182.

[44] Zarabozo-Hurtado, D., González-Garrido, A. A., Guàrdia-Olmos, J., Gómez-Velazquez, F. R., and Peró-Cebollero, M. (2014). Estudio de neuroimagen en sujetos con baja competencia ortográfica ante tareas ortográficas con errores homófonos. *Anuario de Psicología*, In press.